

# EFFECTS OF $K_2CO_3$ AND $Ca(OH)_2$ ON $CO_2$ GASIFICATION OF CHAR WITH HIGH ALKALI AND ALKALINE EARTH METAL CONTENT AND STUDY OF DIFFERENT KINETIC MODELS

Xin YANG<sup>1</sup>, Zhanwei LIANG<sup>2,\*</sup>, Hongwei CHEN<sup>3</sup>, Jixuan WANG<sup>1</sup> and Xinglong MU<sup>3</sup>

<sup>1</sup>School of Water Conservancy and Electric Power, Hebei University of Engineering, Handan City, Hebei, China

<sup>2</sup>Shenhua Guohua (Beijing) Electric Research Institute Co., Ltd., Beijing, China

<sup>3</sup>Key Laboratory of Condition Monitoring and Control for Power Plant Equipment, North China Electric Power University, China

\* Corresponding author; E-mail: hbgcdxyx@163.com

*The  $CO_2$  gasification of South Open-pit Mines coal from Zhundong Field of China using  $Ca(OH)_2$  or  $K_2CO_3$  as catalyst with different loading methods and contents were conducted in thermogravimetric analysis. Comparison of the gasification reactivity and rate of coal loaded various concentration of  $Ca(OH)_2$  concluded that the increase of  $Ca(OH)_2$  loading pronouncedly improved the reactivity and rate for grinding method; nevertheless, for impregnation and high pressure method the increase of  $Ca(OH)_2$  loading observed a similar catalytic effect on char gasification. However, the catalytic effect of  $K_2CO_3$  revealed that the catalytic activity increased with the increase of  $K_2CO_3$  loading for three loading method. For the same catalyst loading, the highest catalytic gasification reactivity achieved for  $Ca(OH)_2$  and  $K_2CO_3$  were the loading methods of high pressure and grinding, respectively. In addition, the gasification of raw char,  $K_2CO_3$  loaded char and  $Ca(OH)_2$  loaded char were quantitatively evaluated by kinetic analysis using shrinking core, random pore and modified random pore models.*

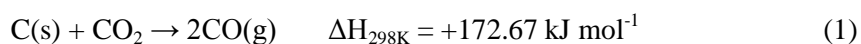
*Key words:  $CO_2$  gasification, catalytic effect, kinetic model, alkali metal, alkaline earth metal*

## 1. Introduction

In the old days, coal and other solid fuels such as biomass were inefficiently utilized only for heat and power generation by conventional combustion. In contrast, the gasification of chars and biomass is an advanced technology which is defined as the thermochemical processes of synthesizing products that allows more clean and efficient use of coal and biomass in form of liquid fuels or syngas. For that reasons, there are numerous researches, using  $H_2O$ ,  $CO_2$  or mixture of both as gasifying agents [1-5], to study char gasification reactions for products of syngas which mainly composes of carbon monoxide (CO) and hydrogen ( $H_2$ ) [6,7].

$CO_2$  gasification of chars, as shown in Eq. (1), has been intensively studied in recent years. On the one hand, the gasification reactivity varied in different types of coals. Bituminous coal char

gasification with CO<sub>2</sub> has been measured by Salatino et al. at gasification and pyrolysis/annealing temperatures ranging from 1173 K to 1473 K and 1173 K to 2273 K respectively. They confirmed that the time/temperature history of the coal samples affected strongly on the gasification reactivity, but barely on the apparent gasification activation energy [8]. Ochoa et al. characterized the CO<sub>2</sub> gasification of two different low-rank coals from Argentina at reaction temperature ranging from 1173 K to 1433 K, and analyzed the effect of experimental operating conditions on char textural and structural features which finally influenced chars gasification [9]. On the other hand, experimental operating conditions have also significant influence on gasification reactivity. Fouga et al. analyzed the influence of different factors such as CO<sub>2</sub> flow rate, sample mass and reaction temperature on reaction rate, and finally determined the factors value in order to establish chemically controlled gasification reaction process [10]. Summarily, both prepared temperature and pyrolysis time of char influenced gasification reactivity to an extent. Liu et al. investigated the influences of total pressure and steam partial pressure upon gasification reactivity of metallurgical coke [11]. They found that the activation energies evaluated under various pressures are alike.



According to the analysis above, the influence of different operation factors, such as pyrolysis and gasification temperatures, sample mass, and CO<sub>2</sub> flow rate, on chars gasification rate varied widely for different types of coals. Thus, it is important to firstly study the influence of experimental condition on special char gasification reactivity.

Catalytic gasification is one of the main techniques due to its high efficiency, availability, low cost and operating temperature. Therefore, there were numerous early investigations on catalytic gasification of different types chars in a stream of CO<sub>2</sub> with different kinds of alkaline metal as catalyst, especially using potassium and calcium salts as catalyst [12]. A Chinese high-rank bituminous coal was used by Xu et al. to study the effects of alkaline metal on coal gasification [13]. Using Na<sub>2</sub>CO<sub>3</sub> as a catalyst, Ding et al. carried out catalytic pyrolysis and gasification experiments, and found that the yields of H<sub>2</sub> and CO increased with the additive amount of Na<sub>2</sub>CO<sub>3</sub> increase from 0 to 15 % at the pyrolysis temperature range of 923-1073 K [14]. Therefore, the effects of two important factors, such as the amounts of catalyst loading and types of carbonaceous material, on the catalytic gasification process must be simultaneously considered.

Catalytic gasification of a Wyodak sub-bituminous coal from the Powder River Basin using Na<sub>2</sub>CO<sub>3</sub> as catalyst was investigated by Popa et al. to evaluate the influence of the factors, such as feed gas composition, catalyst loading amount and reaction temperature on both coal pyrolysis and char gasification processes [15]. For purpose of enhancing catalysis of K<sub>2</sub>CO<sub>3</sub> for steam gasification, Wang et al. proposed mitigating the potassium deactivation in the K<sub>2</sub>CO<sub>3</sub> catalyzed gasification of coal char by adding Ca(OH)<sub>2</sub>, and experimentally found that the reactivity of Ca(OH)<sub>2</sub>-added char was higher than raw char [16]. Through the interactions of K<sub>2</sub>CO<sub>3</sub> with ash-free coal in N<sub>2</sub> or CO<sub>2</sub> atmospheres at 973 K, Kopyscinski et al. found that K<sub>2</sub>CO<sub>3</sub> reduction process was necessary to achieve a fast char conversion and also showed that CO<sub>2</sub> inhibits the process [17]. Li et al. reported that the catalytic effect of K<sub>2</sub>CO<sub>3</sub> was greater than that of Na<sub>2</sub>CO<sub>3</sub> from gasifying Wu Tai gas coal char with CO<sub>2</sub> [18]. Moreover, compared to the other potassium salts, the CO<sub>3</sub><sup>2-</sup> contained in K<sub>2</sub>CO<sub>3</sub> is less harmful than SO<sub>4</sub><sup>2-</sup>, NO<sub>3</sub><sup>-</sup> and Cl<sup>-</sup> to gasification equipment and to environment [19].

Based on above analysis, the gasification reactivity determined from these non-catalytic and catalytic reactions of char are different. In addition, the gasification of coals mined from different

fields vary widely in reactivity, and there are few studies, using  $K_2CO_3$  or  $Ca(OH)_2$  as catalyst loaded with different content and methods, on high alkali and alkaline earth metals coal. Thus, it is essential to investigate the gasification reactivity under several of reaction conditions. In this work, the char gasification with  $CO_2$  using  $Ca(OH)_2$  and  $K_2CO_3$  as catalysts was studied, and the influence of the catalyst loading and addition methods on the gasification reactivity was explored to investigate the catalytic gasification characteristics. Based on detailed comparison of the fitting results of different models, we achieved excellent success in describing non-catalytic and catalytic gasification of the char.

## 2. Experimental

### 2.1. Materials

A South Open-pit Mines coal from Zhundong field located in Xinjiang province belongs to low-rank coal, which is characterized by low mining cost, easy burning out, high reactivity and content of alkali metal. Its properties are shown in Table 1. The powdery  $K_2CO_3$  ( $\geq 99\%$  pure) and  $Ca(OH)_2$  ( $\geq 95\%$  pure) using as gasification catalysts. The purity of  $CO_2$  and  $N_2$  is 99.99% respectively.

**Table 1. Proximate and ultimate analysis of South Open-pit Mines coal**

Proximate analysis/mass%				Ultimate analysis/mass %				$Q_{ar,net}$	
$M_{ar}$	$FC_{ar}$	$V_{ar}$	$A_{ar}$	$C_d$	$H_d$	$N_d$	$O_d$	$S_d$	$MJ\ kg^{-1}$
30.70	41.62	24.63	3.05	77.53	3.86	0.72	12.76	0.53	19.15
Ash composition /mass %									
$SiO_2$	$Al_2O_3$	$Fe_2O_3$	$CaO$	$MgO$	$TiO_2$	$SO_3$	$K_2O$	$Na_2O$	
6.12	8.16	9.37	33.45	5.42	0.41	29.34	0.45	7.28	

ar: As received basis; d: As dry basis; net: Net heating value.

### 2.2. Sample preparation

The coal sample was dried at 378 K for more than 6 h. After cooling down, the coal was taken out, and then pulverized and sieved to obtain a powder of smaller than 160  $\mu m$  in the particle diameter and stored in sealed bottles which were capped to isolate the sample from air.

For brevity, the pyrolysis product of coal sample prepared without catalyst is named the raw char and with catalyst of  $K_2CO_3$  and  $Ca(OH)_2$  are named the PC-char and CH-char, respectively. The catalyst loading is referred to as the weight percent of catalyst in the total amount of the catalyst/coal mixture. The  $K_2CO_3$  loading was 3.2% and 5.0%, the weight percentage was 1.7% and 3.2% for  $Ca(OH)_2$  loading. Catalysts loading in the coal varied in weight to study the effect of catalyst loading on the char gasification rate.

In preparation of the different loading PC-char and CH-char, three loading methods, grinding, impregnation and high pressure method, were used to study the effect of catalyst loading method on char gasification rate. The three methods were described as following. Grinding method: The accurately weighed amount of coal sample and catalyst was thoroughly mixed using mortar and pestle for approximately 20 min at room temperature. The resulting mixture after grinding was dried at 378 K for 12 h to constant mass and stored in air-tight receptacles to prevent further changes.

Impregnation method: Specific quantities of the catalyst were dissolved in a glass beaker using 100 ml deionized water. Then, the coal sample was immersed in the prepared catalyst solution and stirred 40 min with stirred rate of 800 r min<sup>-1</sup>. The resulting mixtures were also dried at 378 K for 12 h to constant mass and stored in air-tight receptacles to prevent further changes.

High pressure method: Initially, a certain amount of the catalyst and coal were dissolved in a reaction kettle body using 30 ml deionized water. Furthermore, the prepared reaction kettle was placed in a collector-type thermostat heating magnetic stirrer and maintained isothermally for 20 min after reaching the target temperature (523 K) and pressure (2.7 MPa). Finally, the resulting solution from the reaction kettle body was also dried at 378 K for 12 h to constant mass and stored in a way as above mentioned.

### 2.3. Experimental equipment and setup

The gasification experiments were performed in a TA Instruments SDT Q600 thermogravimetric analyzer which has a sensitivity of  $\pm 0.1 \mu\text{g}$  for the maximum weight of 200 mg while operating temperature under 1773 K at a heating rate from 0.1 to 100 K min<sup>-1</sup>. The mass flow meter was used to control the flow rate of gas. During the char gasification with CO<sub>2</sub>, the relative mass change of the sample was continuously recorded by the data acquisition system.

To avoid the interparticle and intraparticle diffusion, the experiments were performed in different sample weight (7.5, 10, 12.5 mg), gas flow rate (80, 100, 120 mL/min), and particle size (80, 120, 160  $\mu\text{m}$ ) for the determining of the certain value. Finally, the sample weight of 10 mg ( $\pm 0.05$  mg), gas flow rate of 100 mL min<sup>-1</sup>, and the particle size of 160  $\mu\text{m}$  was obtained. Under this experimental condition, the gasification kinetics proved to be chemical controlled and the combined intraparticle and interparticle diffusion can not affect the overall gasification rate.

The experimental procedure is described briefly as follows: The prepared coal sample was heated from 308 K to the predetermined pyrolysis temperature (1023 K, 1073 K, or 1123 K) at different heating rate (20 K min<sup>-1</sup>, 40 K min<sup>-1</sup>, or 60 K min<sup>-1</sup>) in a N<sub>2</sub> atmosphere. After reaching the desired pyrolysis temperature, the sample was maintained isothermally with N<sub>2</sub> for a certain pyrolysis time (7.5 min, 30 min, or 60 min) and then the gas was switched to CO<sub>2</sub> for isothermal gasification when the temperature reached to gasification temperature of 1023 K. If the pyrolysis temperature is higher than 1023 K, the reactor is cooled down to 1023 K for gasification.

## 3. Results and discussion

The carbon conversion  $X$  is defined as the ratio of the carbon gasified mass at time  $t$  to the total mass changed from the carbon initially gasified to that finally unchanged, as given below:

$$X(t) = \frac{m_0 - m(t)}{m_0 - m_f} \quad (2)$$

where  $m_0$  represents the initial weight of char or the weight at the initial time of gasification,  $m(t)$  is the instantaneous mass of char at gasification time  $t$ , and  $m_f$  is the residual weight of char as it finally unchanged with the gasification time continuing. The gasification rate  $r$  is defined as:

$$r = \frac{dX}{dt} \quad (3)$$

### 3.1. Raw char gasification

There is significant influence of several parameters involved in the pyrolysis on gasification reactivity during the char preparation [20]. Thus, it is most important to determine the pyrolysis parameters of holding time, pyrolysis temperature, and heating rate before conducting the other experiments. Fig. 1 shows typical results of the CO<sub>2</sub> gasification of the raw char at 1023 K with different pyrolysis condition. The holding time of raw coal is defined as the time of raw coal stayed at the temperature of 1023 K in N<sub>2</sub> atmosphere when the pyrolysis temperature reached 1023 K at heating rate of 40 K min<sup>-1</sup>. Similarly, the pyrolysis temperature is defined as the temperature of raw coal isothermally pyrolyzed for 30 min under a stream of N<sub>2</sub> when the predetermined pyrolysis temperature is reached at heating rare of 40 K min<sup>-1</sup>. The heating rate is referred to the increase amount pyrolysis temperature per min.

The data of experiments was seen in Fig. 1(a) that the raw char gasification rate increased with the pyrolysis time from 7.5 min to 30 min, however further expanding the time of isothermal pyrolysis, the gasification rate exhibited decline at all range of char conversion. The latter trend is agreement with that obtained by Liu who illustrated that a longer pyrolysis time result in lower reactivity of a char ascribed to a structure change of the char during pyrolysis and this effect leveled off gradually as pyrolysis time increased [11].

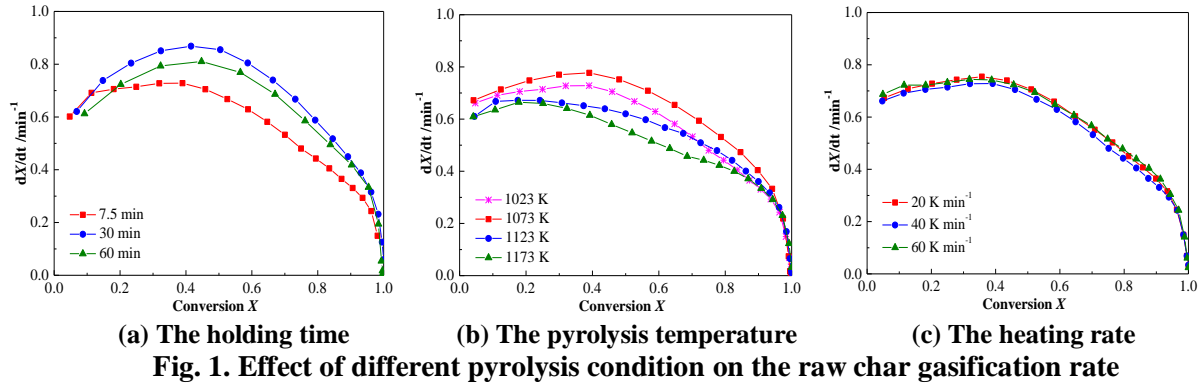
Fig. 1(b) shows the char gasification rate dependence of pyrolysis temperature. It was observed that the raw char gasification rate increased with the pyrolysis temperature increasing from 1023 K to 1073 K, and then declined significantly when further increasing of the pyrolysis temperature. The behavior of reaction rate curves obtained at different pyrolysis temperature may be due to two competing factors concerned with char's structure evolution during coal pyrolysis: pore growth and collapse [21, 22]. Char gasification rate for the 1073 K pyrolysis temperature was highest over almost the whole range of conversion, which is attributed to active sites concentration and the transportation of gas reactant to them, associated with specific surface area, the porosity value and pore size distribution. Thus, in the case of 800 °C pyrolysis, structural and textural feature indicated better performance of char gasification than the others.

The effect of heating rate on raw char gasification rate is illustrated in Fig. 1(c). It is observed that the raw char gasification rate slightly increase at low conversion and then decline significantly to the almost same value at conversion of 0.93 for different heating rate. However, changing the heating rate from 20 K min<sup>-1</sup> to 60 K min<sup>-1</sup> has little effect on the char gasification rate. According above analysis, it can be concluded that the raw char used for gasification experiment was obtain in the pyrolysis conditions of heating rare of 40 K min<sup>-1</sup> to 1073 K pyrolysis temperature for 30 min under a stream of N<sub>2</sub>.

## **3.2. Catalytic gasification**

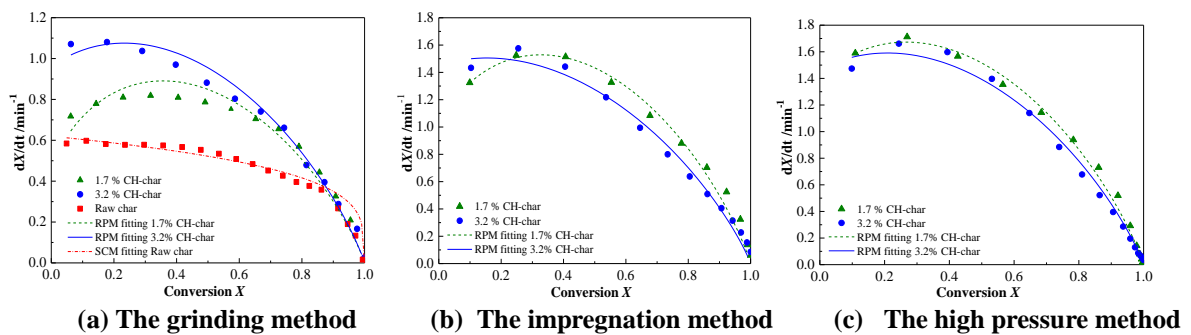
### *3.2.1 Calcium hydroxide catalysis*

The catalytic effect of Ca(OH)<sub>2</sub> with different loading content and methods on gasification rate is shown in Fig. 2. The gasification rate of the raw char without any catalysts was also illustrated in the Fig. 2(a), and it is extremely slow compared with catalytic gasification rate. Whereas for the CH-char, the gasification rate increase until the carbon conversion reached about 0.2 as showed in Fig. 2(a), and then it declined significantly to the same level as raw char at carbon conversion of 1.



The addition of 3.2%  $\text{Ca}(\text{OH})_2$  to coal led to a faster gasification than the addition of 1.7% with grinding method (Fig. 2(a)). The alkaline metal bonded to coal matrix and fixed upon BSUs (Basic Structural Units) would destroy the parallelism of the layer inside the BSUs and the constancy of the interlayer spacing, which inhibited the graphitization process of char during pyrolysis [13, 23]. The carbon crystallite structure was changed by the addition of  $\text{Ca}(\text{OH})_2$  and made carbon more reactive resulting on the higher reactivity of char than the raw char.

However, the experimental data of 3.2% CH-char shown in Fig. 2(b) and (c) were almost superimposed to those for the gasification rate of the 1.7% CH-char, indicating that further increase of the  $\text{Ca}(\text{OH})_2$  loading had little effect on the gasification rate for impregnation and high pressure methods. That because of the carbon surface was coated with a film of  $\text{Ca}(\text{OH})_2$  and then the kinetics would be prevented by the diffusion of the gaseous reactant across the film of  $\text{Ca}(\text{OH})_2$  which reduced the overall reaction reactivity [24]. In more detail, the fine  $\text{Ca}(\text{OH})_2$  particles formed at 1.7%  $\text{Ca}(\text{OH})_2$  loading had high mobility and activity, which could improve the gasification of char. Further increase of  $\text{Ca}(\text{OH})_2$  loading to 3.2% led to the reduction of catalytic gasification rate because of the particle size of  $\text{Ca}(\text{OH})_2$  rising with the increase of  $\text{Ca}(\text{OH})_2$  loading. The high pressure adding method achieved the greatest promotion towards the gasification and the highest gasification rate was of 1.7  $\text{min}^{-1}$  at the conversion of about 0.3. It is almost three times of raw char gasification rate.



The reactivity index  $R_s$  showed in Eq. (4) was generally used to evaluate the gasification reactivity of char, and  $\tau_{0.5}$  is the time at which the carbon conversion ( $X$ ) reaches 0.5. The  $R_s$  values can be calculated from the char conversion  $X$  vs. time  $t$  relationship.

$$R_s = \frac{0.5}{\tau_{0.5}} \quad (4)$$

The reactivity indexes of different chars were presented in Fig. 3 to compare the gasification reactivity of chars prepared with three loading methods of  $\text{Ca}(\text{OH})_2$ . It is seen from the Fig. 3 that the reactivity order of different methods to addition catalyst is: high pressure > impregnation > grinding. This order certainly agreed with the gasification rate order showed in Fig. 2.

The coal incorporate with 3.2%  $\text{Ca}(\text{OH})_2$  had a slightly higher reactivity than the coal with 1.7% in all the three loading methods. This trend is in accord with the gasification rate for grinding method presented in Fig. 2(a), but not in agreement with the rate for impregnation and high pressure methods in Fig. 2(b) and (c). However, although there is slightly different trend between reactivity indexes and the gasification rates for impregnation and high pressure methods, it does not change the main tendency and also can conclude that further increase of the  $\text{Ca}(\text{OH})_2$  has little catalytic effect on gasification reaction.

The comparison of the reactivity indexes for raw char and catalyst loaded chars shows that the reactivity index of raw char is far smaller than those of catalyst loaded ones. It means that the gasification reactivity of the former is lower than those of latter, which achieves much the same result as presenting in Fig.2 that the gasification rate of the raw char is much lower than all the char loading with catalyst.

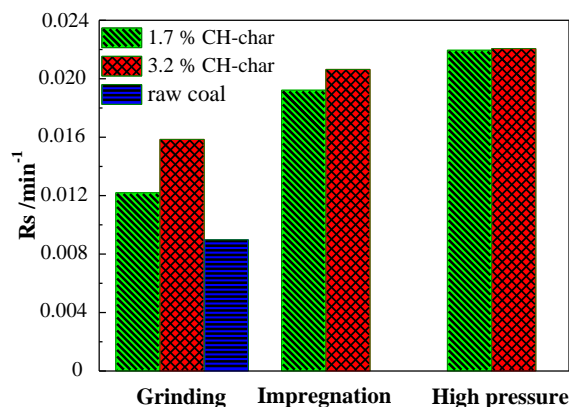


**Fig. 3. The gasification reactivity index of different chars for three loading methods of  $\text{Ca}(\text{OH})_2$**

### 3.2.2 Potassium carbonate catalysis

Fig. 4 showed the effect of  $\text{K}_2\text{CO}_3$  loading on the carbon conversion rate during  $\text{CO}_2$ -char gasification. As observed in these figures, the carbon conversion rate of catalyzed coal was higher than that of raw char showed in Fig. 2(a). The rate increased with the rise of catalyst loading from 3.2% to 5.0% for all the three addition methods. The pure potassium carbonate powder, as showed in Fig. 4(a), has no weight loss at the same condition as char gasification, which could exclude the influence of its weight loss on the  $\text{K}_2\text{CO}_3$  loaded char gasification.

Alkaline metal hindered the progress of carbon graphitization causing the formation of a more reactive char of less ordered crystalline carbon structure during pyrolysis process, which was necessary to make for char gasification [13]. However, in contrast to CH-char, the gasification rate of PC-char was slightly increased in a carbon conversion range of 0-0.6, and then reached to maximum rate in the high conversion range of  $X > 0.5$ . There are recent works to explain the different characteristics of potassium-catalyzed gasification reaction compared to that of calcium [25-26]. Among these explanations, the most acceptable mechanism proposed by Wigmans et al. [27] was the maximum rate obtained at high conversion range, which associated with the activation of the intercalated metal phase. With the carbon conversion proceeding, the potassium, trapped in an

intercalate-like structure, was exposed to retake catalytic effect. Based on this mechanism, Zhang et al. [30] deduced a similar mechanism applied to CO<sub>2</sub> gasification system, which appropriately explained why the gasification rate reached maximum in high conversion range.

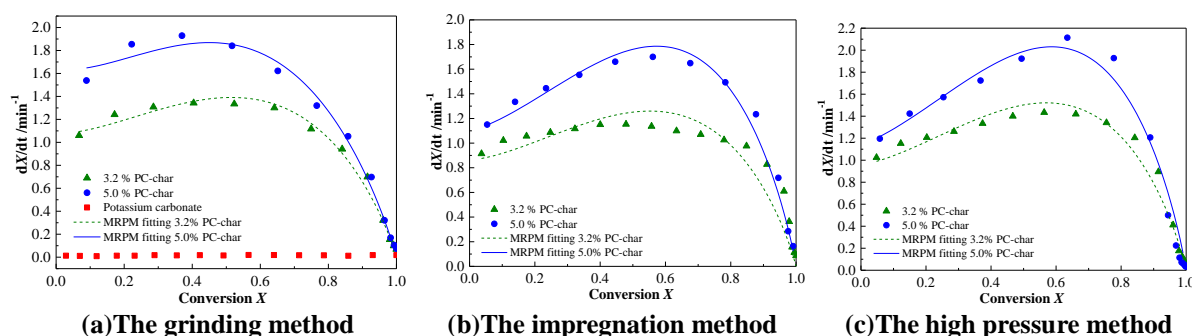


**Fig. 4. The effect of different K<sub>2</sub>CO<sub>3</sub> loading on gasification rate with three addition method**

Here, the average conversion rate is defined as the total conversion of char divided by the used time, which could explain the reactivity of char gasification in whole range of reaction. The bigger of the average conversion rate the higher the reactivity. As presenting in Fig. 5(a), the grinding method of loading catalyst used shorter time to finish the gasification reaction than the other two methods, which means that the average conversion rate of grinding method was higher than the other methods. Therefore, the result could be obtained from the Fig. 5 that the gasification reactivity followed the order: grinding > high pressure > impregnation. It also could be obtained by comparing the two graphs that the char gasification with 3.2% catalyst loading spent longer time than that with 5.0%, thus the average conversion rate was smaller for the char with 3.2% catalyst. Consequently, the gasification reactivity was enhanced with the increase of K<sub>2</sub>CO<sub>3</sub> loading from the amounts of 3.2% to 5.0%.

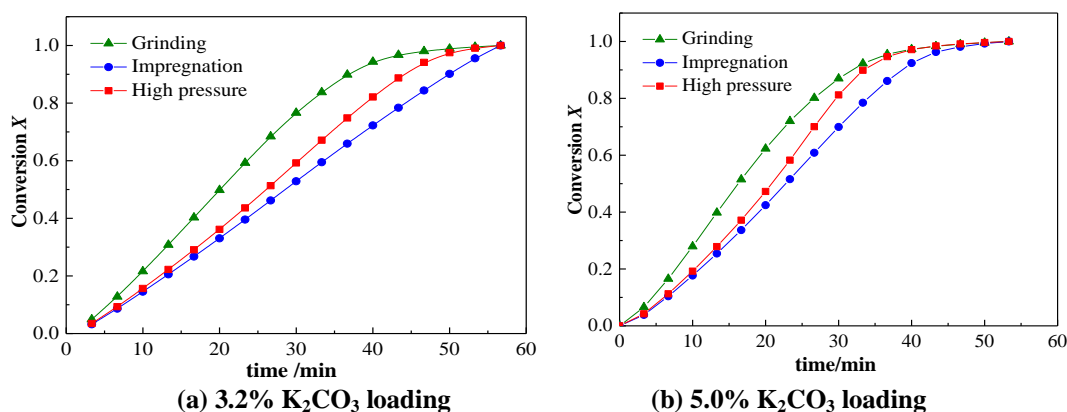


**Fig. 5. X-t curves for different K<sub>2</sub>CO<sub>3</sub> loading using three methods**

A comparison of reactivity indexes between 3.2% and 5.0% K<sub>2</sub>CO<sub>3</sub> loading using different addition methods was conducted. It can be seen from Fig.6 that the reactivity indexes of different catalyst loaded methods during CO<sub>2</sub> gasification followed the order: grinding > high pressure > impregnation, which was agreement with the average conversion rate illustrated in Fig. 5. The Fig. 6 also showed that the reactivity index increased with the catalyst addition for all the three loading methods. The more catalyst loading correspond to higher reactivity index, as the result of comparing the two graphs of Fig. 5 to obtain a larger average conversion rate for more catalyst loading.



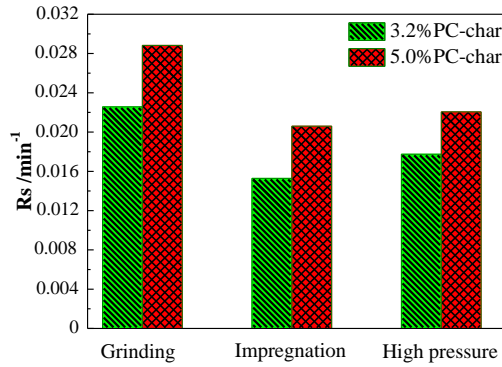


**Fig. 6. The gasification reactivity index of different chars for three loading methods of  $K_2CO_3$**

### 3.3. Kinetic models

#### 3.3.1 Model fitting

The purpose of kinetic modeling is to use simple equations to predict the chemical reaction process. Four models representing the chemical reaction kinetics of gasification have received more attention in recent years and are discussed elsewhere [28, 29]. The homogeneous model (Hom) is the simplest and assumes that the gasifying agents react with active sites at both inside and outside the particle surface [30]. This model is described as:

$$\frac{dX}{dt} = k_H(1 - X) \quad (5)$$

where  $k_H$  is the carbon conversion rate constant for homogeneous model.

The shrinking core model (SCM) assumes that the reaction occurs either on exterior of the char particle or within external pores of particle surface, and gradually moves toward the center, leaving ash layer behind [Error! Bookmark not defined., 31]. At intermediate conversion of the solid, there is a shrinking core of the unreacted solid, which diminishes as the reaction proceeds [Error! Bookmark not defined.]. The model is described as:

$$\frac{dX}{dt} = k_S(1 - X)^m \quad (6)$$

where  $k_S$  is the carbon conversion rate constant for shrinking core model, and  $m$  is a shape factor.

The random pore model (RPM), developed by Bhatia et al. [28], take into account the pore texture of the char particle and its evolution during gasification. It assumes that the reaction is carried out in the internal surface of the pore structure and that the cylindrical pores enlarge as the internal surfaces erode with the proceeding of the reaction, eventually merging with each other [Error! Bookmark not defined., 31]. The basic expression was given by:

$$\frac{dX}{dt} = k_R(1 - X)\sqrt{1 - \psi \ln(1 - X)} \quad (7)$$

Two basic characteristic parameters contained in the model were the reaction rate constant  $k_R$ , and the dimensionless structural parameter  $\psi$ . By differentiation of Eq. (7),  $\psi$  can be obtained in terms of  $X_{\max}$  as follow [28]:

$$\psi = \frac{2}{2 \ln(1 - X_{\max}) + 1} \quad (8)$$

The modified random pore model (MRPM) proposed by Zhang et al. [29, 30] was established to predict the gasification rate incorporating a maximum in the high conversion range, predominately attribute to the catalytic effect of the potassium. As indicated below:

$$\frac{dX}{dt} = k_M(1-X)\sqrt{1-\psi \ln(1-X)}(1+\theta^p) \quad (9)$$

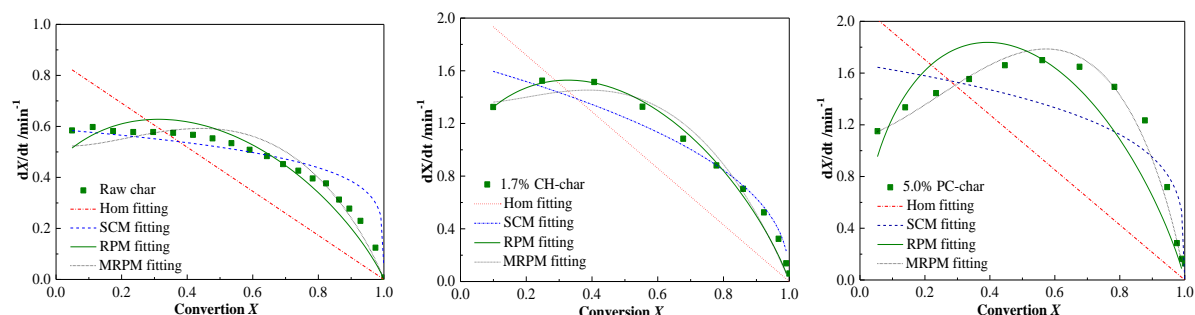
where  $\theta=cX$  or  $c(1-X)$  corresponds to two different reactivity patterns with maximum rate in the low or high conversion range, respectively.  $k_M$  is the reaction rate constant,  $\psi$  is same as in Eq. (7),  $\theta$  is a variable function,  $c$  and  $p$  are empirical constants.

For determining the suitability of the four models to experimental data, fitting results for the experimental data collected from raw char, 1.7% CH-char in impregnation method, and 5.0% PC-char in impregnation method are exhibited in Fig. 7. As observed from Fig. 7(a), it can be seen that the raw char experimental data was best fitted by SCM, the other models cannot correctly fit the raw char experimental data from the conversion of 0 to 1. For 1.7% CH-char in impregnation method, as illustrating in Fig. 7(b), it showed that the best fitting model is RPM, which can well-describe the experimental data of CH-char in impregnation sample. The satisfactorily fitting model for 5.0% PC-char in impregnation method is MRPM comparing to the other models as presenting in Fig. 7(c).

From Fig. 7(b), it can be concluded that the coal sample loaded by  $\text{Ca}(\text{OH})_2$  with impregnation method is well fitted by RPM, thus the 1.7% and 3.2% CH-char samples with three loading methods of grinding, impregnation and high pressure were all be fitted by RPM, which is illustrated in Fig. 2. It can be seen from Fig. 2(a),  $\text{Ca}(\text{OH})_2$  loaded with grinding method, that the RPM underestimate the experimental data for both 1.7% and 3.2% CH-char at carbon conversion higher than 0.8, but the RPM can describe the experimental data trend at carbon conversion smaller than 0.8. For both 1.7% and 3.2% CH-char in impregnation and high pressure method, the 1.7% CH-char sample is well described by the RPM at all range of carbon conversion, and the 3.2% CH-char sample is also well described by the RPM at carbon conversion of higher than 0.2, but at the carbon conversion lower than 0.2 the RPM fitness of experimental data has some deviation.

The MRPM fitness of 3.2% and 5.0% PC-char samples in three different loading methods is illustrated in Fig. 4. Fig. 4(b) shows that the values of MRPM overestimate the experimental data at carbon conversion of 0.5-0.7 for the two samples in impregnation loading method. For 3.2% and 5.0% PC-char samples in grinding and high pressure method, the MRPM can well fit the experimental data in all range of carbon conversion.

Summarily, although there are some minor deviations between the model prediction and the experimental data, this degree of deviation is considered acceptable and it can illustrate applicability of models performance for the experimental data. Therefore, it can be concluded that the raw char, CH-char and PC-char are able to be described by SCM, RPM, MRPM, respectively.



(a) The raw char                      (b) 1.7% CH-char                      (c) 3.2% PC-char.

**Fig. 7. The models fitted the experimental data obtained from different types of char**

### 3.3.2 Activation energy

The four models aforementioned can be simplified as the following expression:

$$\frac{dX}{dt} = kf(X) \quad (10)$$

By integrating Eq. (10), the integral expression can be rearranged as the following:

$$F(X) = kt \quad (11)$$

where  $F(X)$  is the integral expression of  $1/f(X)$ .

The reaction rate constants ( $k$ ) at different temperatures (750, 800 and 850°C) can be obtained from plots of  $F(X)$  vs.  $t$ , as illustrating in Fig. 8, and the linear correlation coefficient of Fig. 8 was showed in Supplementary Information. According to the Arrhenius equation:

$$k = k_0 e^{-E_a/RT} \quad (12)$$

The activation energy  $E_a$  included in the Arrhenius equation can be calculated from the slope of the logarithm of reaction rate constant ( $\ln k$ ) vs. reciprocal of the absolute temperature ( $1/T$ ), which was showed in Fig. 9, and the linear correlation coefficient of Fig. 9 was presented in Supplementary Information. The results of activation energies obtained from SCM, RPM and MRPM are listed in Table 2.

**Table 2. Activation energies of SCM, RPM, MRPM and ICM**

		Raw char	CH-char	PC-char
$E_a$ KJ mol <sup>-1</sup>	SCM	120±12		
	RPM		58±4	
	MRPM			81±6
	ICM	80±7~118±11	44±5~75±9	72±13~116±16

Isoconversion method (ICM), as presented elsewhere [33], is defined as a free-model approach to calculate activation energy at a particular conversion, which allows to determine accuracy of the most common kinetic models used in gasification at temperatures lower than 1273 K by comparing the value of the activation energy estimated in kinetic models with that of the free model calculation.

As presenting in Eq. (12), the  $k$  is then substituted into the Eq. (11) and applied natural logarithms to obtain the following equation:

$$\ln t = \ln \frac{F(X)}{k_0} + \frac{E_a}{R} \frac{1}{T} \quad (13)$$

where  $R$  is the gas constant; the first term on the right-hand side of Eq. (13) is a function of carbon conversion. For a given  $X$ , the time ( $t$ ) to attain the  $X$  corresponds to a certain temperature, such as 1023, 1073 and 1123 K, and then the activation energy can be obtained from the slope of the plot  $\ln t$  vs.  $1/T$ , which was showed in Fig. 10, and the linear correlation coefficient of Fig. 10 was illustrated in Supplementary Information.

In this study, using a free-model approach at three different temperatures of 1023 K, 1073 K, and 1123 K, the activation energy is obtained independent of the kinetic model for different conversion from 0.1 to 0.9 with an interval of 0.1. The results of activation energy calculated by ICM for three types of coals are presented in Table 2. It can be seen that the activation energy calculated at a lower

conversion is smaller than at a higher conversion. There are recent works on activation energy related to different conversion that attempt to explain the activation energy increases with conversion rather than constant and independent of the conversion [34, 35]. This trend is mainly due to the reduction or deactivation of catalysts obtained by Gomez et al. [35].

Comparing the activation energies achieved from the three models with that calculated by model-free method, it can be seen that the activation energies obtained from the models are in the range of model-free values, respectively. It means that, in the aspect of activation energy, the three models can well describe the three types of chars, respectively.

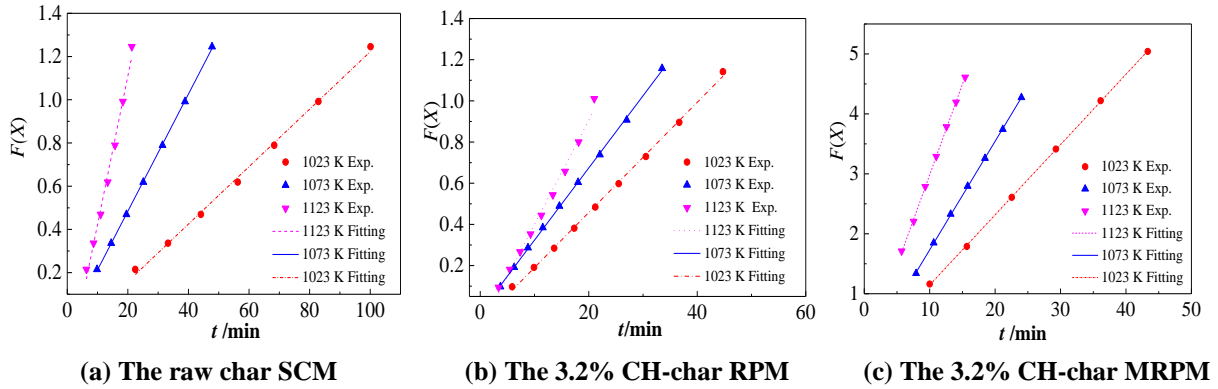


Fig. 8. Plots of  $F(X)$  vs.  $t$  at different temperatures

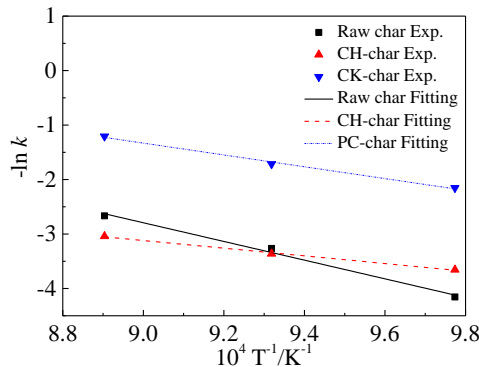


Fig. 9. Plot of  $\ln k$  vs.  $1/T$  at different char samples

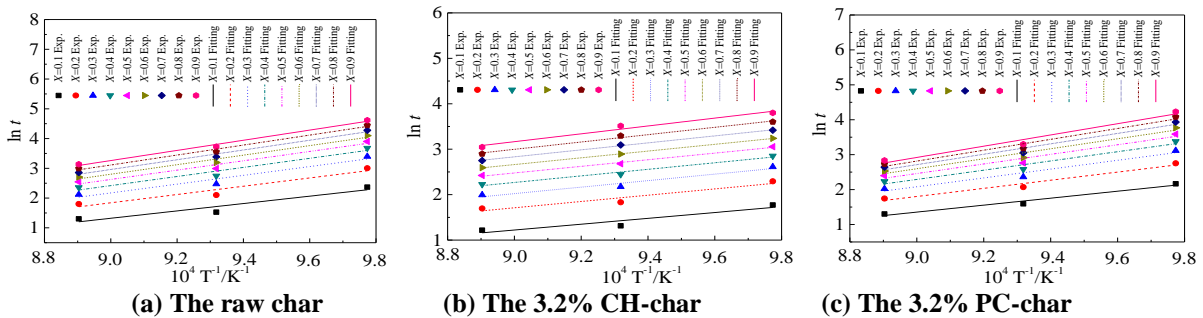


Fig. 10. Plots of  $\ln t$  vs.  $1/T$  for different conversions  $X$

#### 4. Conclusions

The raw coal gasification with  $\text{CO}_2$  under various of pyrolysis conditions were conducted and finally obtained that the best holding time and temperature were 30 min and 800 °C, respectively. For  $\text{Ca}(\text{OH})_2$  loaded with grinding method, the catalytic effect was promoted as increasing the  $\text{Ca}(\text{OH})_2$

loading. There was no difference on catalytic effect for impregnation and high pressure method when increasing  $\text{Ca}(\text{OH})_2$  loading from 1.7% to 3.2%. However, the gasification reactivity significantly improved as increasing  $\text{K}_2\text{CO}_3$  loading for all the three loading methods. For the same  $\text{Ca}(\text{OH})_2$  loading, the catalytic activity of the three loading method followed the sequence of high pressure > impregnation > grinding, while the gasification reactivity of char with the same  $\text{K}_2\text{CO}_3$  loading followed the order: grinding > high pressure > impregnation. The raw char, CH-char and PC-char were well-describe by shrinking core, random pore and modified random pore model, respectively. Simultaneously, the activation energy achieved from the aforementioned models was in agreement with that of free model calculation.

## Acknowledgement

This project was supported by The Research Foundation of Education Bureau of Hebei Province of China (No. ZD2020182).

## References

- [1] Roberts, D., Harris, D., Char gasification in mixture of  $\text{CO}_2$  and  $\text{H}_2\text{O}$ : competition and inhibition, *Fuel*, 86 (2007), pp. 2672-2678
- [2] Tremel, A., *et al.*, Experimental investigation of high temperature and high pressure coal gasification, *Applied Energy*, 92 (2012), pp. 279-285
- [3] Prabowo, B., *et al.*,  $\text{CO}_2$ -steam mixture for direct and indirect gasification of rice straw in a downdraft gasifier: laboratory-scale experiments and performance prediction, *Applied Energy*, 113 (2014), pp. 670-679
- [4] Wen, C., *et al.*, The pyrolysis and gasification performances of waste textile under carbon dioxide atmosphere, *Journal of Thermal Analysis and Calorimetry*, 128 (2017), pp. 581-591
- [5] Yang, Z., *et al.*, Identification for the behavior of maximum reaction rate during the initial stage of coal char gasification, *Journal of Thermal Analysis and Calorimetry*, 128 (2017), pp. 1186-1194
- [6] Grigore, M., *et al.*, Mineral reactions during coal gasification with carbon dioxide, *International Journal of Coal Geology*, 75 (2008), pp. 213-224
- [7] Zhang, F., *et al.*,  $\text{CO}_2$  gasification of Powder River Basin coal catalyzed by a cost-effective and environmentally friendly iron catalyst, *Applied Energy*, 145 (2015), pp. 295-305
- [8] Salatino, P., *et al.*, Assessment of thermodeactivation during gasification of a bituminous coal char, *Energy Fuels*, 13 (1999), pp. 1154-1159
- [9] Ochoa, J., *et al.*,  $\text{CO}_2$  gasification of Argentinean coal chars: a kinetic characterization, *Fuel Processing Technology*, 74 (2001), pp. 161-171
- [10] Fouga, G., *et al.*, Kinetic study of Argentinean asphaltite gasification using carbon dioxide as gasifying agent, *Fuel*, 90 (2011), pp. 674-680
- [11] Liu, Z., Wang, Q., Kinetic study on metallurgical coke gasification by steam under various pressure, *Journal of Thermal Analysis and Calorimetry*, 129 (2017), pp: 1839-1845
- [12] Fernandez, L., *et al.*, Kinetic study of the  $\text{CO}_2$  gasification of manure samples, *Journal of Thermal Analysis and Calorimetry*, 129 (2017), pp. 2499-2509
- [13] Xu, S., *et al.*, Effects of alkaline metal on coal gasification at pyrolysis and gasification phases, *Fuel*, 90 (2011), pp. 1723-1730
- [14] Ding, L., *et al.*, Catalytic effects of  $\text{Na}_2\text{CO}_3$  additive on coal pyrolysis and gasification, *Fuel*, 142 (2015), pp. 134-144
- [15] Popa, T., *et al.*, Catalytic gasification of a Powder River Basin coal, *Fuel*, 103 (2013), pp. 161-170
- [16] Wang, J., *et al.*, Enhanced catalysis of  $\text{K}_2\text{CO}_3$  for steam gasification of coal char by using  $\text{Ca}(\text{OH})_2$  in char preparation, *Fuel*, 89 (2010), pp. 310-317
- [17] Kopyscinski, J., *et al.*,  $\text{K}_2\text{CO}_3$  catalyzed  $\text{CO}_2$  gasification of ash-free coal. Interactions of the

- catalyst with carbon in N<sub>2</sub> and CO<sub>2</sub> atmosphere, *Fuel*, 117 (2014), pp. 1181-1189
- [18] Li, S., Cheng, Y., Catalytic gasification of gas-coal char in CO<sub>2</sub>, *Fuel*, 74 (1995), pp. 456-458
- [19] Popa, T., *et al.*, H<sub>2</sub> and CO<sub>x</sub> generation from coal gasification catalyzed by a cost-effective iron catalyst, *Applied Catalysis A, General*, 464-465(2013), pp. 207-217
- [20] Ahmed, I., Gupta, A., Kinetics of woodchips char gasification with steam and carbon dioxide, *Applied Energy*, 88 (2011), pp. 1613-1619
- [21] Reyes, S., Jensen, K., Modeling of catalytic char gasification. *Industrial and Engineering Chemistry Research Fundamentals*, 23 (1984), pp. 223-229.
- [22] Zolin, A., *et al.*, A comparison of coal char reactivity determined from thermogravimetric and laminar flow reactor experiments, *Energy Fuels*, 12 (1998), pp. 268-276
- [23] Hayashi, J., *et al.*, Roles of inherent metallic species in secondary reactions of tar and char during rapid pyrolysis of brown coals in a drop tube reactor, *Fuel*, 81 (2002), pp. 1977-1987
- [24] Wang, Y., *et al.*, Investigation into the characteristics of Na<sub>2</sub>CO<sub>3</sub>-catalyzed steam gasification for a high-aluminum coal char, *Journal of Thermal Analysis and Calorimetry*, 131 (2018), pp. 1213-1220
- [25] Marquez, M., *et al.*, CO<sub>2</sub> and steam gasification of a grapefruit skin char, *Fuel*, 81 (2002), pp. 423-429
- [26] Moulijn, J., Kapteijn, F., Towards a unified theory of reaction of carbon with oxygen-containing molecules, *Carbon*, 33 (1995), 8, pp. 1155-1165
- [27] Wigmans, T., *et al.*, The influence of pretreatment conditions on the activity and stability of sodium and potassium catalysts in carbon-steam reactions, *Carbon*, 21 (1995), 3, pp. 295-301
- [28] Bhatia, S., Perlmutter, D., A random pore model for fluid-solid reaction. 1. Isothermal, kinetic control, *AIChE Journal*, 26 (1980), 3, pp. 379-386
- [29] Zhang, Y., *et al.*, Proposal of a semi-empirical kinetic model to reconcile with gasification reactivity profiles of biomass chars, *Fuel*, 87 (2008), pp. 475-481
- [30] Zhang, Y., *et al.*, Modeling of catalytic gasification kinetics of coal char and carbon, *Fuel*, 89 (2010), pp. 152-157
- [31] Homma, S., *et al.*, Gas-solid reaction model for a shrinking spherical particle with unreacted shrinking core, *Chemical Engineering Science*, 60 (2005), pp. 4971-4980
- [32] Zhang, L., *et al.*, Gasification reactivity and kinetics of typical Chinese anthracite chars with steam and CO<sub>2</sub>, *Energy Fuels*, 20 (2006), pp. 1201-1210
- [33] Flynn, J., Thermal analysis kinetics-problems, pitfalls and how to deal with them, *Journal of Thermal Analysis*, 34 (1988), pp. 367-381
- [34] Demicco, G., *et al.*, Kinetics of the gasification of a Rio Turbio coal under different pyrolysis temperatures, *Fuel*, 95 (2012), pp. 537-543.
- [35] Gomez, A., Mahinpey, N., Kinetic study of coal steam and CO<sub>2</sub> gasification: A new method to reduce interparticle diffusion, *Fuel*, 148 (2015), pp. 160-167

Submitted: 11.08.2020.

Revised: 19.09.2020.

Accepted: 22.09.2020.